



Chirplet Wigner–Ville distribution for time–frequency representation and its application



G. Chen*, J. Chen, G.M. Dong

State Key Laboratory of Mechanical System and Vibration, Shanghai Jiao Tong University, NO. 800 Dongchuan Road, Minhang District, Shanghai, China

ARTICLE INFO

Article history:

Received 7 June 2013

Received in revised form

9 August 2013

Accepted 13 August 2013

Available online 5 September 2013

Keywords:

Time–frequency analysis

Cross-term

Wigner–Ville distribution

Polynomials Chirplet transform

Spline Chirplet transform

Echolocation signal analysis

ABSTRACT

This paper presents a Chirplet Wigner–Ville Distribution (CWVD) that is free for cross-term that usually occurs in Wigner–Ville distribution (WVD). By transforming the signal with frequency rotating operators, several mono-frequency signals without intermittent are obtained, WVD is applied to the rotated signals that is cross-term free, then some frequency shift operators corresponding to the rotating operator are utilized to relocate the signal's instantaneous frequencies (IFs). The operators' parameters come from the estimation of the IFs which are approached with a polynomial functions or spline functions. What is more, by analysis of error, the main factors for the performance of the novel method have been discovered and an effective signal extending method based on the IFs estimation has been developed to improve the energy concentration of WVD. The excellent performance of the novel method was manifested by applying it to estimate the IFs of some numerical signals and the echolocation signal emitted by the Large Brown Bat.

© 2013 Elsevier Ltd. All rights reserved.

1. Introduction

In signal processing, time–frequency representation (TFR)-based approaches have raised a variety of vital applications in mechanical fault diagnosis [1], electronic system [2], geotechnical [3], biomedical engineering [4], etc., in which various TFR methods have been applied to extract meaningful physical parameters or patterns from the original signals. The main work of getting precise parameters or patterns is obtaining the precise instantaneous frequency (IF) whose concept was put forward by Carson and Fry first [5] and improved by Van der Pol [6], Boashash provided a comprehensive overview for the various IF estimation methods [7,8].

1.1. Brief introduction of TFR methods

To get the precise IF, the TFR methods' energy concentrating ability at and around the IF must be taken into consideration. During the last half century since the coming out of Cooley and Tukey's fast Fourier transform [9], the TFR methods have entered a rapid development period especially in conducting the nonlinearity, no-stationary signals. Recalling the development trajectory of TFR methods, there are some approaches that have aroused considerable interest among researchers. Those approaches, namely, the Short Time Fourier Transform (STFT) and the Wavelet Transform (WT) are

* Corresponding author. Tel.: +86 158 0075 0723.

E-mail addresses: stevenchen@sjtu.edu.cn, megangchen@gmail.com (G. Chen).

widely used for TFR. However, as restricted by the Heisenberg uncertainty principle that the time resolution Δt and the frequency resolution Δf satisfy the inequality $\Delta t \Delta f > = 1/4\pi$, the STFT could not obtain a high resolution in time and frequency simultaneously as the trade-off between them is an inevitable problem. In addition, the fixed window width of STFT makes it impossible to meet the requirement that we need a high time resolution in high frequency band and a high frequency resolution in low frequency band in many cases. This shortage leads to the development of WT. As WT is thrived from STFT, it cannot achieve a high-precision estimation for time varying IFs as well.

Among the TFR methods, the Empirical Mode Decomposition (EMD) that works in temporal space directly instead of corresponding frequency space [10] is a new way for TFR, so as to the atomic decompositions (AD) [11] that also decomposes the original signal into atomic models and can estimate and match the local structure of signal quite well. Unfortunately, due to EMD's adaptive and empirical nature as well as its sensitivity to the changing of parameters, for instance the stopping criterion, choice of interpolation, and also to local signal variations caused by added noise [12], signals that share similar statistics often emerge different decompositions both in terms of their properties and their number by EMD. What is more, the model mixing phenomenon [13], the fast algorithm, the construction of atoms' module base etc. are still unsolved problems for atomic decomposition method.

Meanwhile, the WVD whose kernel is equal to 1 is a very popular TFR method that is a kind of bilinear transformation and can achieve an excellent energy concentration for noise-free signals. However, when nonlinear frequency or intermittent signal components are contained in the analytical signal, cross-term will occur to contaminate the original signal and lead to misunderstanding. Attracted by WVD's excellent performance in TFR, considerable attention has been paid to the suppression of cross-term in the last three decades, such as the pseudo-WVD [14,15], beam-forming [16], EMD-based [17] etc.. However, the pseudo-WVD which adds a window to the analysis signal makes the WVD degenerate into "Window" method and the EMD-based method makes the WVD degenerate into "decomposition" method which introduces more error sources. In general, these methods for cross-term suppression in some way have suppressed the good performance of WVD when suppress the cross-term at the same time.

1.2. Chirplet transform

The Chirplet transform is the generalization form of fast Fourier Transform, short-time Fourier transform, and wavelet transform [18]. As having the most flexible time frequency window, it has been successfully used in practices. For instance, Guo-Sheng and Feng-Feng used the Chirplet transform for harmonics detection [18], Millioz and Davies applied it to FMCW radar signals [19], Kerber et al. used Chirplet Transform for attenuation analysis of lamb waves [20] etc.

The Chirplet transform is an expansion of an arbitrary function onto a basis of multi-scale chirps [21]. For a frequency-modulated signal $x(t) \in L^2(\mathbb{R})$, its CT at τ is defined as

$$CT(\tau, \omega, \alpha; \sigma) = \int_{-\infty}^{+\infty} z(t) e^{-j(\alpha/2)(t-\tau)^2} \omega_\sigma(t-\tau) e^{-j\omega t} dt \quad (1)$$

where $z(t)$ is the analytical signal of $x(t)$, coming from the Hilbert transform \mathbf{H} , i.e., $z(t) = x(t) + jH[x(t)]$, and the definition of Hilbert transform can be rewritten as follow

$$x_h(t) = x(t) \otimes h(t) = \int_{-\infty}^{+\infty} x(\tau) h(t-\tau) d\tau = \frac{1}{\pi} \int_{-\infty}^{+\infty} \frac{x(\tau)}{t-\tau} d\tau \quad (2)$$

Eq. (2) showed that the signal after Hilbert transform $x_h(t)$ is equal to the output signal from a filter with transfer function $H(f)$ which is the Fourier transform of $h(t)$. $H(f)$ can be defined as

$$H(f) = -j \operatorname{sgn}(f) = \begin{cases} -j & \text{if } f \geq 0 \\ j & \text{if } f \leq 0 \end{cases} \quad (3)$$

This Hilbert transform exists for all functions of class L^p (see, for example, Titchmarsh 1948). With this definition, the analytical signal, $z(t)$, can be rewritten as

$$z(t) = x(t) + jH[x(t)] = a(t) e^{j\theta(t)} \quad (4)$$

in which

$$a(t) = \sqrt{x(t)^2 + H[x(t)]^2} \quad \theta(t) = \arctan\left(\frac{H[x(t)]}{x(t)}\right)$$

In Eq. (1), τ and α are the local time and frequency respectively, and $\omega_\sigma(t)$ is a symmetric, nonnegative, and normalized real window which is often taken as the Gaussian window defined as

$$\omega_\sigma(t) = \frac{1}{\sqrt{2\pi}\sigma} e^{-(1/2)(t/\sigma)^2} \quad (5)$$

The Chirplet transform defined by (1) can be interpreted as the STFT of the analytical signal multiplied by a complex window function, from which the Chirplet transform can be rewritten as [22]

$$CT(\tau, \omega, \alpha; \sigma) = \int_{-\infty}^{+\infty} z(t)\phi^R(t, \tau, \alpha)\phi^S(t, \tau, \alpha)\omega_\sigma(t-\tau)e^{-j\omega t} dt \quad (6)$$

where

$$\begin{cases} \phi^R(t, \alpha) = \exp(-jat^2/2) \\ \phi^S(t, \tau) = \exp(j\alpha\tau t) \end{cases} \quad (7)$$

Obviously, the $\phi^R(t, \alpha)$ is a frequency rotating operator which rotates the analytical signal $z(t)$ by an angle of $\arctan(-\alpha)$ in the time–frequency plane and the $\phi^S(t, \tau)$ is the frequency shift operator that relocates the frequency component at ω to $\omega + \alpha\tau$. What is more, from (7), the Chirplet transform is a kind of parameterized time–frequency transform.

In order to get the accurate time–frequency representation for nonlinear, non-stationary signal, the TFR methods mentioned above cannot meet the requirement clearly. Conventionally, the parameterized time–frequency transform is used to analyze the linear–frequency–modulated (LFM) signals [23] or nonlinear–frequency–modulated (NLFM) signal [24], while to the LFM and NLFM mixed signals, the previous methods show the lack of efficiency and accuracy. Faced with these problems, the authors of this paper take advantage of the WVD's excellent resolution in time and frequency, and a parameterized time–frequency transform that can also be called polynomial or Spline Chirplet transform has been developed to suppress the cross-term. This paper's layout is as follows. Section 2 is an introduction of the novel method and some comparative study has been discussed. Section 3 shows the algorithms of time–frequency image contour recognition and parameter identification of frequency–rotating and frequency–shift operators. In Section 4, the good performance of the novel method is demonstrated by a numerical experiment test and a set of vibration signal came from a rotor test rig, the conclusions are seen in Section 5.

2. The novel method

2.1. WVD

WVD is a typical representative of Cohen's class of Bilinear TFRs with kernel $\phi(t, \omega) = 1$ that has been widely used. It can be defined as

$$WVD(t, \omega) = \int_{-\infty}^{+\infty} x\left(t + \frac{\tau}{2}\right) \times x\left(t - \frac{\tau}{2}\right) e^{-j\omega\tau} d\tau \quad (8)$$

In Eq. (8), when $x(t)$ is a mono-frequency signal, the result will be perfect, while when the analysis signal is the sum of two or more signal components, i.e. $x(t) + y(t)$, then we have

$$WVD_{x+y}(t, \omega) = WVD_x(t, \omega) + 2\text{Re}[WVD_{x,y}(t, \omega)] + WVD_y(t, \omega) \quad (9)$$

Eq. (9) shows the cross-term $2\text{Re}[WVD_{x,y}(t, \omega)]$ will occur when the analysis signal is not a mono-frequency signal. While for real system, the signal is usually a mixture of many signal components in which the cross-term will come up to reduce the time–frequency resolution or produce false signals that make it difficult to extract the useful information from WVD and cross-term suppression is of a great need.

2.2. Chirplet WVD

The Chirplet transform has many good characteristics, however, it only suit for liner frequency modulate signal. While when combine the Chirplet transform and WVD, the drawbacks of the two methods can be suppressed and the advantages can be highlighted.

The best way to suppress the cross-term in WVD is transforming the non-linear, non-stationary analytical signal into some mono-linear-frequency signals. This paper applies some frequency rotating and frequency shift operators to realize the transformation process whose schematic diagram is showed in Fig. 1. The signal in Fig. 1(a) is the original signal that mixed with a non-linear chirp signal and an intermittent chirp signal as marked by real IF1 and real IF2. The dotted lines in Fig. 1(b) are processed signal IF by the frequency–rotating operator of IF1, and then the IF1 was transformed into a mono-frequency signal. To separate those signals, a band-pass filter was used for this situation and the result was shown in Fig. 1(c) and (d) was the reconstructed signal for IF1 by frequency shift operator and IF2 can be accurately estimated through the same process as IF1. From the process shown above, the definition of the process can also be written as

$$CWVD(t, \omega) = \sum_{i=1}^N \int_{-\infty}^{+\infty} \bar{z}_i\left(t + \frac{v}{2}\right) \times \bar{z}_i\left(t - \frac{v}{2}\right) \phi_i^S(t, \tau, \alpha) e^{-j\omega v} dv \quad (10)$$

With $\bar{z}_i(t) = z(t)\phi_i^R(t, \tau, \alpha)\psi(t, \omega_i)$, $\phi_i^R(t, \tau, \alpha)$ and $\phi_i^S(t, \tau, \alpha)$ are the frequency rotating operator and frequency shift operator, and $\psi(t, \omega_0)$ is a band-pass filter with pass-band frequency of ω_0 .

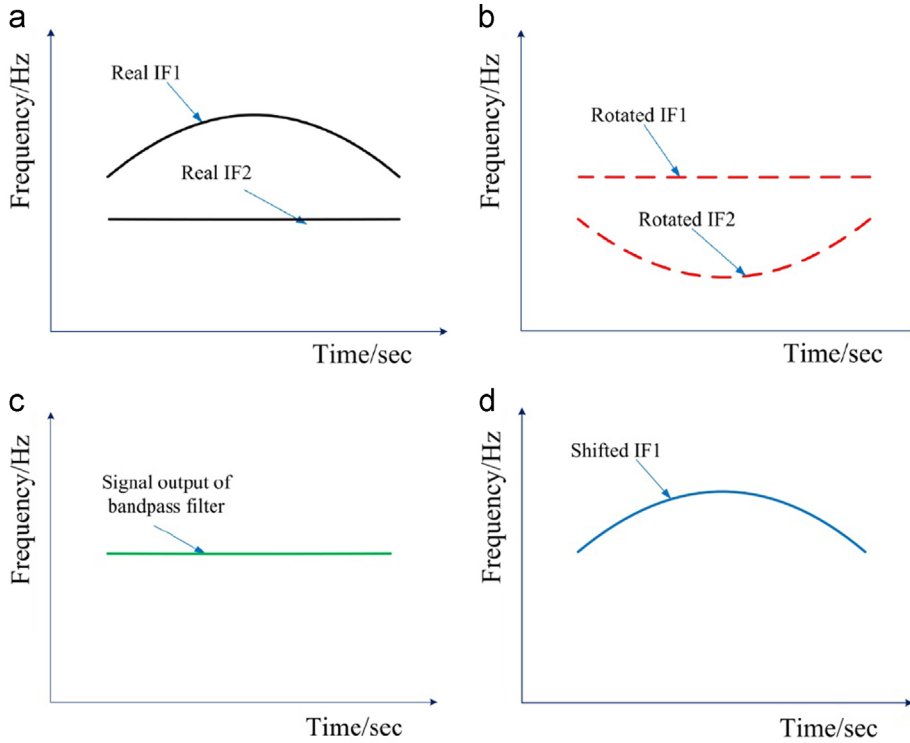


Fig. 1. The novel method's processing procedure schismatic. (a) IFs of the original signal, (b) IFs after frequency rotating process, (c) the band-pass filter's output and (d) IFs after frequency shift process.

For an illustrative purpose of the process, a LFM signal was taken as an example, and the signal can be rewritten as $x(t) = \sin [2\pi(f_0 + (1/2)\alpha t)t]$. Obviously, the IF of the signal is $(f_0 + \alpha t)$, where α is the slope of the analysis signal. In this case, the $\phi_i^R(t, \tau, \alpha)$ rotates the analytical signal $z(t)$ by an angle of $\arctan(-\alpha)$ to make the signal be a mono-frequency signal that is free for cross-term in WVD, and then $\phi_i^S(t, \tau, \alpha)$ relocates the rotated signal by applying a frequency shift of $\alpha\tau$ to reconstruct the signal after WVD is applied. As there is only one signal in the analysis signal, the band-pass filter is not needed in this case. From above, we can see that after frequency rotating and frequency shift, the cross-term suppressed WVD can be obtained.

2.3. Polynomial Chirplet WVD

It is obvious that the frequency rotating and frequency shift operators' parameters depend on the IF estimation of the signal. When the order of polynomial is not very high, the polynomial is a better choice to provide smooth and efficient approximation to continuous function. Here we use some polynomials which can approximation the IFs with low order and the estimation algorithm will be shown in Section 3. The polynomial for one of the signal component can be rewritten as

$$f_i(\tau) = \alpha_0 + \sum_{k=1}^N \alpha_k \tau^k \quad t_0 \leq \tau \leq t_1 \quad (11)$$

where $f_i(t)$ is the IF estimation of the i th signal component and t_0, t_1 are the time boundary of the polynomial.

Obviously, the polynomial function will have the ability to approach the IF's trajectory precisely when the polynomial kernel parameters $(\alpha_0, \alpha_1, \alpha_2, \dots, \alpha_N)$ are estimated properly. To transform the original signal into some mono-continuous-frequency and rehabilitate to original signal, the frequency rotating and frequency shift operator can be rewritten as follows

$$\phi_i^R(t, \tau, \alpha) = \exp\left(-j \sum_{k=0}^n \frac{1}{k+1} \alpha_k \tau^{k+1} + j\lambda t\right) \quad (12)$$

$$\phi_i^S(t, \tau, \alpha) = \exp\left(-2\left(j \sum_{k=1}^{n+1} \alpha_{k-1} \tau^{k-1} t - j\lambda t\right)\right) \quad (13)$$

In Eqs. (12) and (13), the parameter λ is an additional frequency shift that used to match the band-pass filter's pass-band frequency. As the band-pass filter's pass-band is fixed that reduces the computation and improves computational efficiency greatly, the λ is needed to match the constant band-pass filter that also is a constant. To illustrate the frequency rotating and

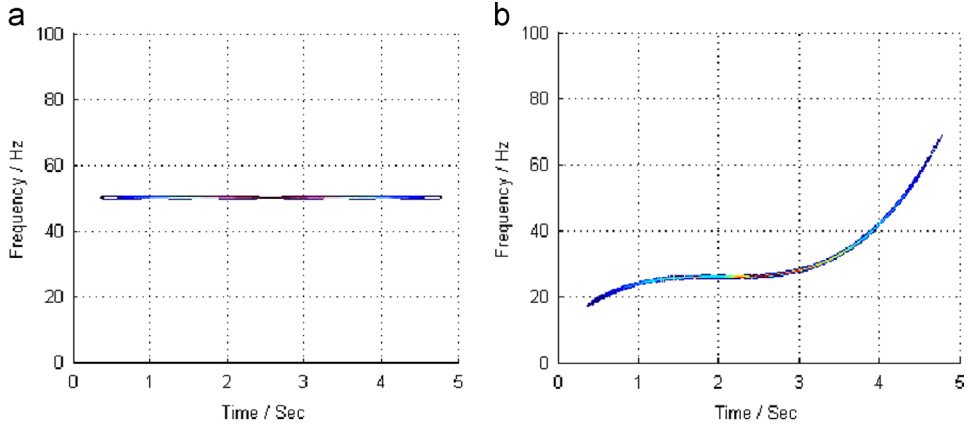


Fig. 2. Contour map for the output. (a) Only frequency rotating operator is applied and (b) frequency rotating and shift operators are applied.

shift clearly and intuitively, a simple signal with one signal component is used to be a demonstration that shown as follows

$$s(t) = \sin\left(2\pi\left(\frac{1}{2}t^4 - 4t^3 + 12t^2 + 10t\right)\right) \quad t \in [0, 5] \quad (14)$$

The signal is sampled with a sampling frequency of 200 Hz, and the IF trajectory of this signal is $f(t) = 2t^3 - 12t^2 + 24t + 10$ (Hz). Then the frequency rotating and frequency shift operator can be given as follows

$$\phi_1^R(t, \tau, \alpha) = \exp\left(-j\left(\frac{1}{2}\tau^4 - 4\tau^3 + 12\tau^2 + 10\tau - 50t\right)\right) \quad \tau \in [0, 5] \quad (15)$$

$$\phi_1^S(t, \tau, \alpha) = \exp(-2j((2\tau^3 - 12\tau^2 + 24\tau - 10)t - 50t)) \quad \tau \in [0, 5] \quad (16)$$

The frequency rotated and shifted WVD is shown in Fig. 2

In Fig. 2(a), the signal defined by Eq. (14) was transformed by the frequency-rotating operator defined by Eq. (15), and the result is a mono-frequency signal. Fig. 2(b) is the outcome of the transformation defined by Eq. (16) that showed the cross-term of WVD has suppressed totally and the exhibited good energy concentration.

2.4. Spline Chirplet WVD

The polynomial Chirplet transform will go into shadow when the order of the polynomial increase as the Gram matrix would be ill-conditioned in solving the least square approximation. What is more, as the increasing of the polynomial order, the computation will increase a lot and Runge phenomenon will occur as showed in Fig. 3(b). To deal with this situation, the spline-kernelled Chirplet transform is utilized as the spline is effective in approximating high dynamic trajectory on a larger interval as showed in Fig. 3(c).

Compared with the polynomial Chirplet WVD (PCWVD), the spline Chirplet WVD (SCWVD) has a little change in the definition of the frequency rotating and frequency shift operator that can be defined as follows

$$\phi_i^R(t, Q) = \exp\left(-j\sum_{k=1}^n \frac{q_k^h}{k}(t-t_h)^k + j\lambda t + \eta_h\right) \quad t \in [t_h, t_{h+1}] \quad (17)$$

$$\phi_i^S(t, \tau, Q) = \exp\left(-2\left(j\sum_{k=1}^n q_k^h(\tau-t_h)^{k-1}t - j\lambda t\right)\right) \quad t \in [t_h, t_{h+1}] \quad (18)$$

where $\phi_i^R(t, Q)$ and $\phi_i^S(t, \tau, Q)$ are frequency rotating and frequency shift operator for time interval $t \in [t_h, t_{h+1}]$ for signal component i respectively. $Q(h, k) = q_k^h$ denotes the local polynomial coefficient matrix of the spline; λ is an added frequency shift as PCWVD showed above. η_h is a boundary constraint for the spline interpolation that satisfies the equation showed below

$$\eta_h - \eta_{h+1} = \sum_{k=1}^n \frac{q_k^{h+1}}{k}(t_h - t_{h+1})^k \quad (19)$$

where $\eta_1 = 0$.

From the definition of the CWVD showed above, the CWVD is a kind of parameterized time–frequency transform that operate the analytical signal in the time–frequency plane. Compared to other time–frequency operation methods, namely, the generalized synchrosqueezing transform (GST) in [25] that the original signal is first mapped in time domain to an analytical signal with a constant frequency to eliminate the time dimensional blur of the TFR then the mapped signal is produced by CWT, so as to the Polynomial Chirplet Transform (PCT) in [22] that also used the frequency rotating and shift

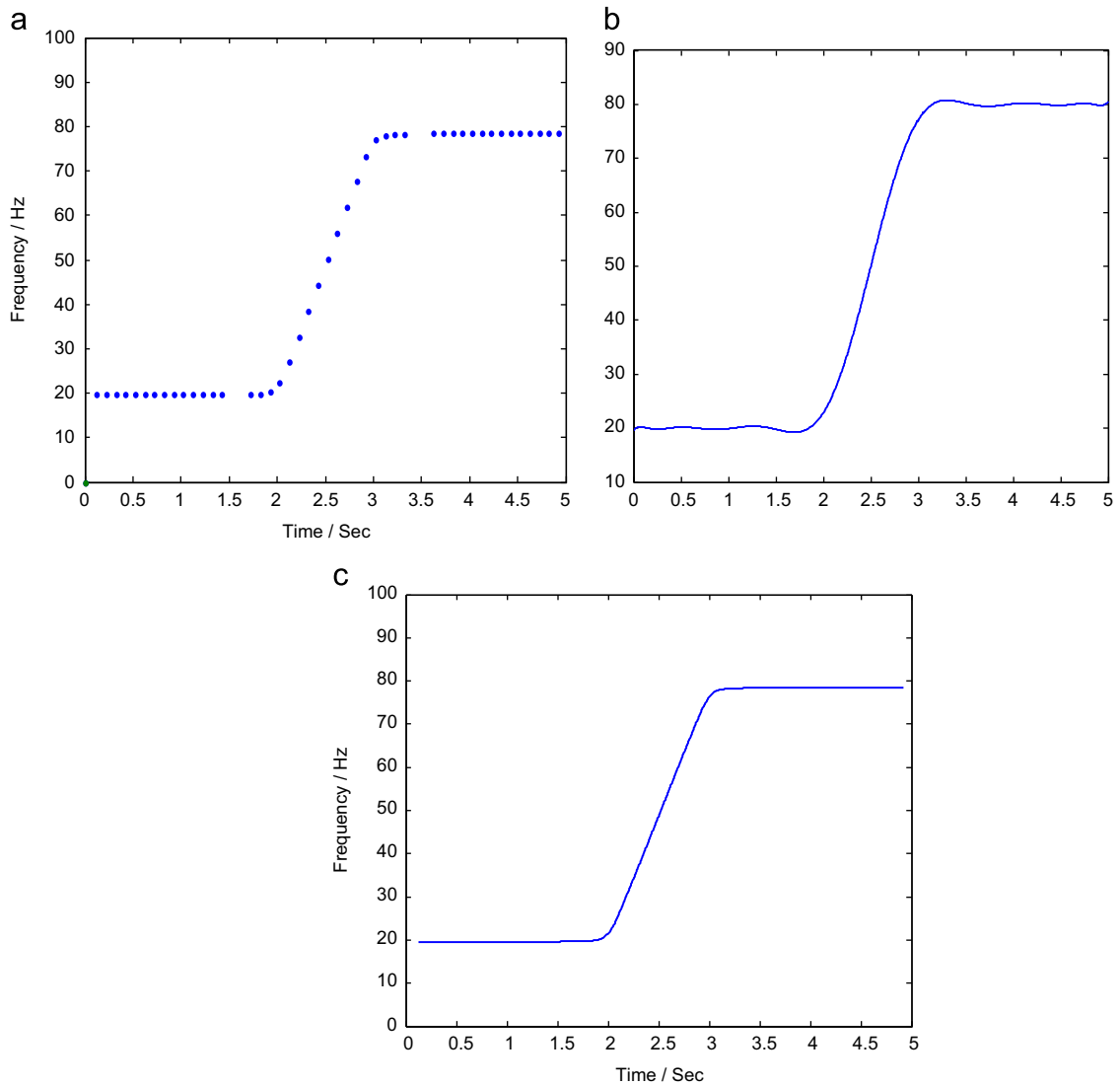


Fig. 3. IFs detection and curve fitting with spline. (a) data classification, (b) curve fitting with a 14 order polynomial and (c) curve fitting with spline.

operator first to transform the original signal and then CWT is applied to the transform signal, the CWVD has its own concerns and strengths. First, Both the GST and PCT transform the operated signal with CWT that limited the frequency resolution as the existence of Heisenberg uncertainty principle. Second, the CWVD is good at improving the energy concentration of the interesting IFs while the GST may have superiority in the mechanical fault diagnosis. Third, the PCT is a time consuming algorithm as the needed of iterative optimization process.

3. Parameter estimation method

The parameters estimation for the polynomial or spline kernel functions that approximate the IFs whose significance is of self-evident and directly determines the efficiency of the novel method's performance. The proposed method in this paper used least squares method to appropriate the IFs of the original signal when the polynomial function's order is less than 15 and the process of the approaching can be divided into two steps that are IFs estimation and polynomial approaching.

IFs estimation algorithm aims at using some polynomial functions to approach the trajectory of the instantaneous frequency of the original signal. In other words, we use some polynomial functions to approach the IFs trajectory that ignore the amplitude of the peaks, consequently, the first job of IFs estimation is peaks detection. In this paper, the STFT is utilized to achieve the roughly IFs before performing the peak detection algorithm as the STFT is simple and perspicuity. After the rough IFs are obtained by STFT, peaks detection will be performed by searching for downward zero-crossings in the smoothed first derivative of each time slice that shown detailed in [26]. In order to prevent interference signal or noise

producing false peaks, an amplitude threshold was used to discriminate the false and true signal that shown as follow

$$A_{th} = 0.1 \times A_{max} \quad (20)$$

where A_{max} is the maximum amplitude of all the IFs peaks and A_{th} is the threshold of the frequency amplitude.

3.1. Data classification

After the peak detection work is finished and the peaks' positions are saved in a matrix, the next step is using some polynomial curves or spline functions to approach all the peaks' trajectory. However, when the signal has many components, only one polynomial curve cannot approach the IFs very well and the Runge phenomenon will arise. Likewise, the data partitioning is needed to classify all the peaks in some groups. This paper uses the contour extraction technique that usually is applied in reverse engineering that can find the trajectory of the IFs intelligently and classify the peaks in some groups, then with each group a polynomial function or spline function can be obtained using least squares method. In reverse engineering, many data partitioning methods can be available such as fuzzy clustering method, Support Vector Machine (SVM) etc. Taking into account the computational efficiency, the classification process for this paper is shown as follow:

- (1) Search the peak matrix and search peaks along the time axis and the length of searching step is 20 points, every 20 sampling points choose one points which is a resampling process, then save the chosen peaks in a new matrix.
- (2) Search the new matrix and find the first peak along the time axis, then classify the found peak into the first group, and set the found peak as the local peak.
- (3) Search the peaks forward the local peak as searching forward can guarantee a one-to-one mapping of the time and frequency, if the found peaks are under the threshold that is a preset curve jerk under the assumption that the curve is smooth to ensure the found point belonging to the same group.
- (4) Step 2 has found many peaks may belong to the same group, and step 3 will determine which point is the best point. In the algorithm, the last two peaks' local slope are calculated and saved, then search for the most likely peaks that coincides with the slope changing trend in the found peaks by step 2, then classify the found peak into the same group and set the found peak as the local point.
- (5) Return to step 3 until any peaks belong to the same group cannot be found.
- (6) Return to step 2 and begin to find peaks belonging to the next group, then return to step 1 until all the peaks have been classified and go to step 5.

The numerical experiment result showed that even though the noise suppression method described by Eq. (12), there are still many noise components after peaks fitting by polynomial function or spline function. To resolve this problem, this paper utilizes a simpler and efficient way that removes the short time signals as short time signals usually generated by the noise signals. This measure we take has reduced the signal components greatly that demonstrated by the simulation result. What is more, the experiment result also demonstrated that the method of removal short time signal is efficient for Gaussian noise. However, the method also showed powerless for many other noises that should be improved when applied to other field.

3.2. Curve fitting

The data classification method showed above has classified the data into some classes, and then the next step is using some polynomial or spline function to approach the frequency trajectory. Before the curve fitting is conducted, there is a trade-off between the computational efficiency and goodness of the fit. Obviously, in many cases, the polynomial function with least square method is more computational efficiency than the spline interpolation. The authors in this paper have set a standard to decide which method should be chosen. The standard can be defined as follow:

$$\delta = \sqrt{\frac{\sum_{i=1}^N (f(x_i) - y_i)^2}{N-1}} < \xi_0 \quad (21)$$

where ξ_0 is the standard deviation threshold for polynomial for fitting and N is the total points in the group. If the standard deviation exceeds the threshold, the spline approximation method is used.

4. Validations

4.1. Numerical experiment test

In order to verify the advantage of the proposed CWVD, this section provides several tests with some numerical signals. For the purpose of comparison, some conventional TFR methods are considered, for instance the STFT, WVD and pseudo-WVD.

To verify the performance of the polynomial CWVD, the numerical signal used in this test is given as follow

$$s_1(t) = \sin\left(2\pi\left(-\frac{4}{3}t_1^3 + 10t_1^2 + 50t_1\right)\right) + \sin(80\pi t_2) + \sin(80\pi t_3)$$

$$0 \leq t_1 \leq 5, 0 \leq t_2 \leq 2, 3 \leq t_3 \leq 5 \quad (22)$$

Obviously, the signal $s_1(t)$ consists of three components and two of them are mono-frequency signal with the same frequency but has been disconnected in time domain. The signal is sampled with a sampling frequency of 200 Hz, and the trajectory of the signal is shown in Fig. 4(e). In Fig. 4(d), the IFs of the signal are extracted by the STFT with a window width of 256, and the instantaneous frequency showed that the STFT method has a very low resolution both in frequency and time domain. In Fig. 4(e), the peaks detection algorithm is applied and also showed the good performance of the algorithm. After the peaks detection process, three curves are fitted with the least square method and the results are shown in Table 1. The parameter estimation result in Table 1 also shows the poor estimation in time domain that affected by the STFT's bad time resolution, especially when the signal is short in time domain. Fig. 4(f) shows the good energy concentration of the proposed method and the novel method has suppressed the cross-term totally, while in Fig. 4(f) the edge blur phenomenon still exists in the novel method that occurs in all existing method including the WT, STFT, EMD etc. and there is not a perfect solution for this problem at present.

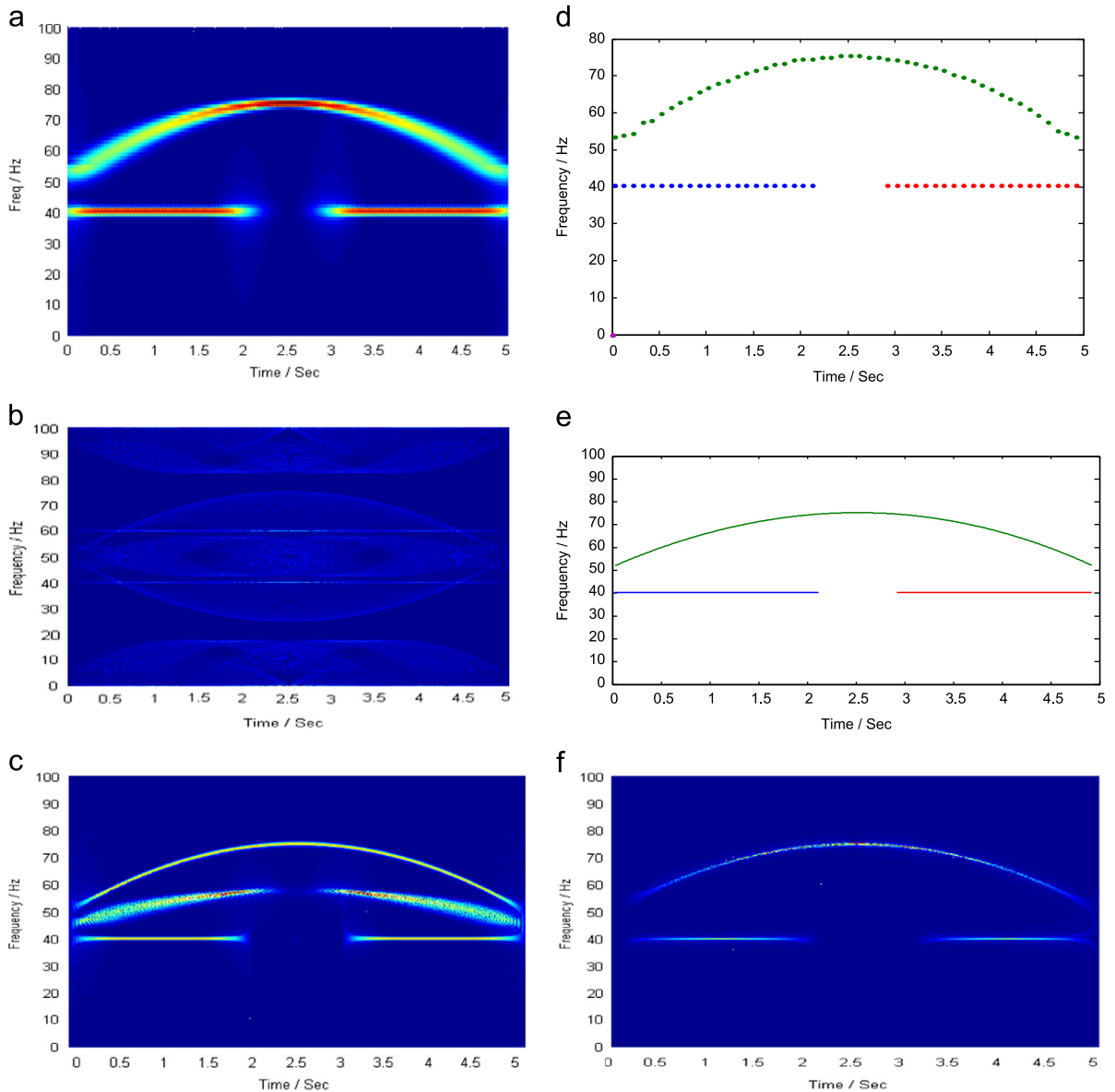


Fig. 4. Test result. (a) By STFT with window width 512, (b) WVD, (c) PWVD with window width 512, (d) data classification result, (e) curve fitting with polynomial function and (f) CWVD.

Table 1
The parameter estimating result.

Curve numbers	α_0 (estimated/real)	α_1 (estimated/real)	α_2 (estimated/real)	α_3 (estimated/real)	Start time (estimated/real)	End time (estimated/real)
1	40.2/40	0/0	0/0	0/0	0/0	2.25/2
2	51.0/50	19.2/20	-3.8/-4	0/0	0/0	5/5
3	0/0	0.49/0	-2.1/0	43/40	3.75/3	5/5

To verify the performance of the spline CWVD, a more complicated numerical signal was generated that is given as follow

$$s_2(t) = \sin(-200 \cos(0.4\pi t) + 100\pi t) + \sin(20\pi t + 16\pi t^2) \quad 0 \leq t \leq 5 \quad (23)$$

In this case, the signal $s_2(t)$ consists of two components. One is a chirping component with the chirp rate of 16 Hz/s and the other with IF law of $\sin(0.4\pi t) + 50$. What is more, a cross of the two components in the time–frequency plane added a challenge to the proposed method. The sampling frequency is 200 Hz and the window length is 512, respectively. The TFR obtained by the STFT, WVD, PWVD, CWVD are shown in Fig. 5.

Thought the comparison of the STFT, WVD, PWVD, CWVD showed in Fig. 5, the energy of STFT's TFR is distributed horizontally all over the time–frequency plane as STFT approximates the IF with a horizontal line. What' worse, compared Fig. 5(a) with Fig. 4(a), when the chirp rate is high, a bad energy concentration will be got. In Fig. 5(b) and Fig. 4(b), the interference component is serious especially in Fig. 5(b), that has led to misunderstandings. The PWVD's TFR in Fig. 5(c) and Fig. 4(c) shows the PWVD has been interfered by the cross-term. Compared Fig. 5(f) and Fig. 4(f) to the others, the good energy concentration ability of the CWVD is self-evident and the CWVD is free for cross-term, respectively.

4.2. Application to echolocation signal

The definition of the CWVD shows that it is essentially kinds of Chirplet transforms which allows for a unified framework for comparison of various time–frequency methods [23]. The numerical test shows that the CWVD is good for IFs, no matter linear or non-linear, estimation with high energy concentration. In this part, the CWVD is applied to the echolocation signal. The digitized 2.5 μ s echolocation pulse emitted by the Large Brown Bat, *Eptesicus Fuscus*. There are 400 samples; the sampling period was 7 μ s (the data is available in [27]). The waveform of the signal is showed in Fig. 6(a). As showed by [28], there are three NLFM components in the echolocation signal. The TFDs obtained by the STFT (with window size 256), PWVD (with window size 256) and the proposed CWVD are shown in Fig. 6(b)–(d). Fig. 6 shows that the STFT has a poor energy concentration along the IFs that makes it be not able to achieve the accurate IF estimation for all components, the PWVD has better IFs estimation accurate while the inevitable cross-term between the three components will lead to misinterpretation of the signal and the CWVD has obtain a higher energy concentration along the IFs trajectory without any cross-terms.

4.3. Error analysis and enhance thinking.

The vital idea of the proposed method is using some polynomials or splines to approach the IFs trajectory and rotate and shift the original signal according to the approached polynomial or spline to transform the non-linear, non-stationary signals into some mono-frequency signals that cross-term will be suppressed in WVD. Generally, the polynomials Chirplet transform's resolution mainly depends on the accuracy of the parameter estimation, therefore for this case, mainly depends on the accuracy of parameters for polynomial. To evaluate the level of error, some criterions are used, and the criterions are defined as follows

$$\xi_1 = \text{mean} \left(\int \frac{|\text{IF}_{\text{estimated}}(t_{In}) - \text{IF}_{\text{real}}(t_{In})|}{|\text{IF}_{\text{real}}(t_{In})|} dt \right) \quad (24)$$

$$\xi_2 = -\iint \log |\text{WVD}_{\text{estimated}}(t, \omega)|^3 dt d\omega \quad (25)$$

Eq. (24) used the estimated IF as a criterion, in Eq. (24) the estimated IFs and real IFs have the same time domain that means that it only focus on the approaching error and ignores the border distortions phenomenon. Eq. (25) used the concentration of the TFD as a criterion and the Renyi entropy is used to evaluate the concentration. To simplify and make the analysis result indicate the effect factor clearly, here just takes the non-linearity component in Eq. (23) into consideration. The three criterion's result for the proposed method is shown in Table 2.

Table 2 shows that the error of the IF estimated is small while the energy concentration of the WVD is not good that gives us a method to improve the performance of the proposed method. In other words, attention should be paid on the improvement of the energy concentration but not the parameter estimation in the proposed method. What is more, the parameter estimation can be improved by using the latest WVD as peak detection's data source to substitute the STFT and then can be enhanced with an iterative process to refining the parameters. When it comes to energy concentration, majority

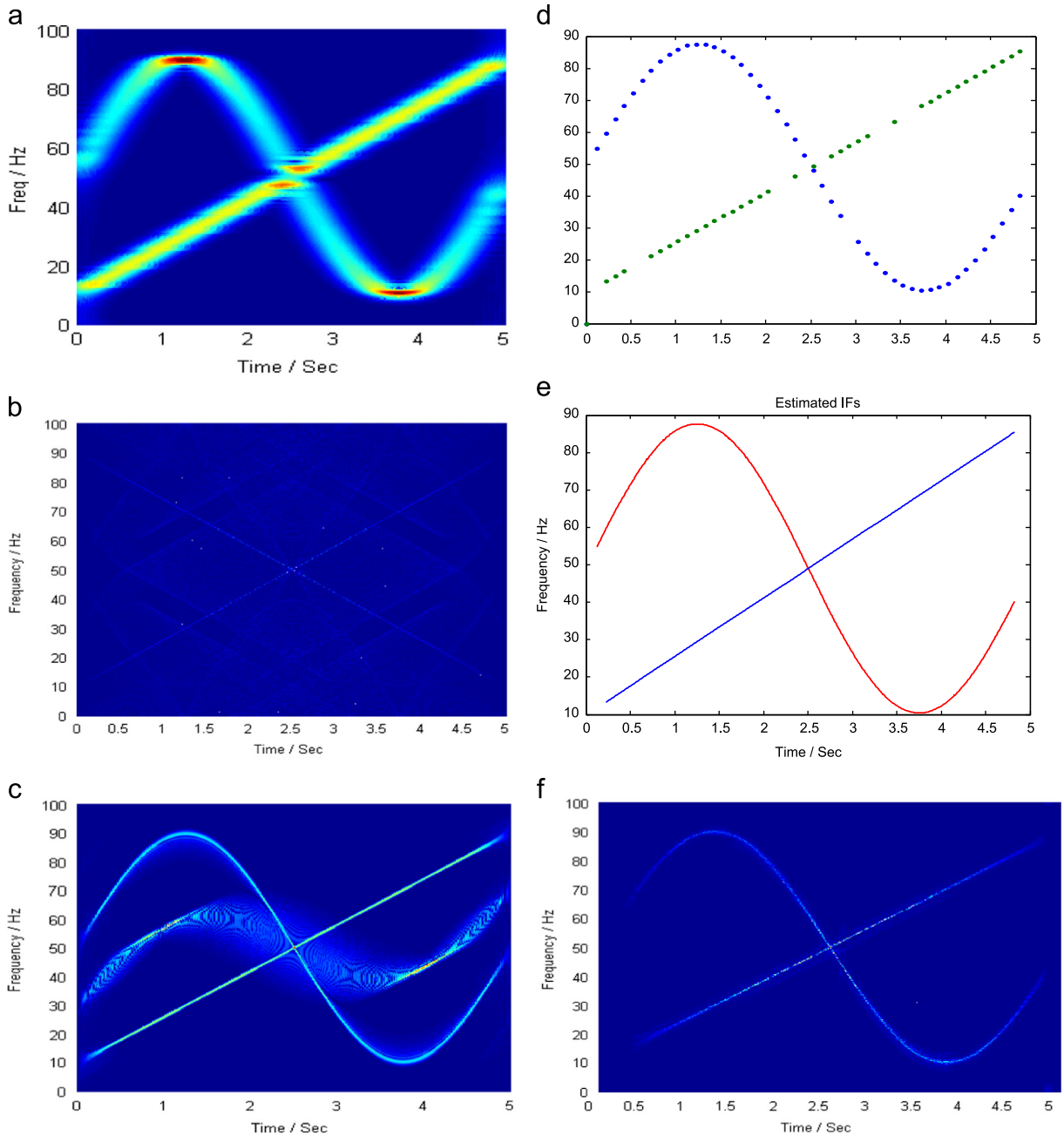


Fig. 5. Test result. (a) STFT with window width 512, (b) WVD, (c) PWVD with window width 512, (d) data classification result, (e) curve fitting with spline and f) CWVD.

error comes from the border distortions that can be improved by signal extending in some way. To demonstrate the effectiveness of the extending method for error reduction, this paper extended the signal through the parameter obtain above to the tested signal and here also just focused on the non-linearity component. Fig. 7 shown the novel method's WVD with a contour map after signal extending was applied and Table 3 showed the estimation error from which the effectiveness of the signal extension in energy concentration can be shown obviously.

5. Conclusion

With the frequency rotating and shift operator, the proposed method has transformed the non-linearity, multi-component, non-station signal into some mono-frequency signal, then the WVD was applied to the transformed signal and

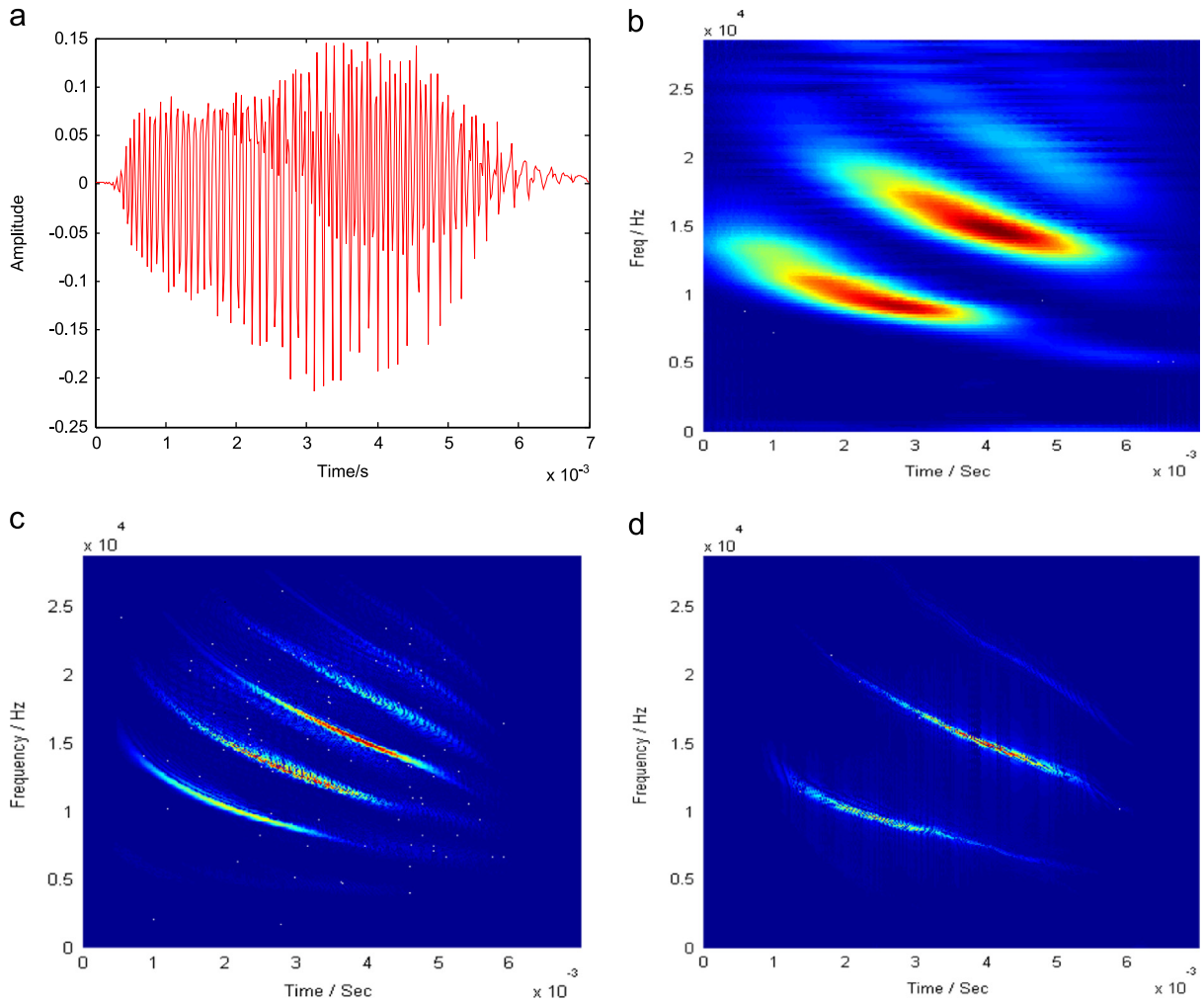


Fig. 6. Frequency estimation with CWVD. (a) waveform, (b) STFT, (c) PWVD and (d) CWVD.

Table 2
Estimation error of the proposed method.

Criterion	ξ_1	ξ_2
Value	2.17%	4.6e5

the cross-term usually exists in WVD has suppressed totally. Compared to the conventional TFR methods, for instance the STFT and WT, the CWVD has taken advantage the WVD's high resolution characteristic and avoided the shortage caused by the cross term of WVD. What is more, the CWVD has broken through the limit of Heisenberg 'uncertainty principle'. However, as the CWVD is a kinds of TFR methods based on Chirplet transform, the large computation makes is difficult to achieve real-time operation which restricts it application in many field such as motor control, real-time measurement etc.

In the proposed method, the data portioning technical will decide the adaptability of the new method and the accuracy of the parameter estimation. Nevertheless, there is no doubt that there are many other techniques may have a better performance in data classification and peaks detection, furthermore, various interpolation methods such as spline interpolation, cubic interpolation etc. or curve fitting methods such as Gaussian approaching, Fourier approaching etc. can be developed to expand the applicability of the proposed method in some certain cases. However, the application experience shows the strong background noise will affect the validity of the method greatly, so the authors of this paper think that more consideration should be paid to the noise separation and distinction, as noise will easily mislead the polynomials approaching process that will restrict the novel method's efficiency. At last, through the analysis of the novel method's error, the impact of the border distortions showed great power in introducing error that has led us to pay more attention to the solution of border distortions.

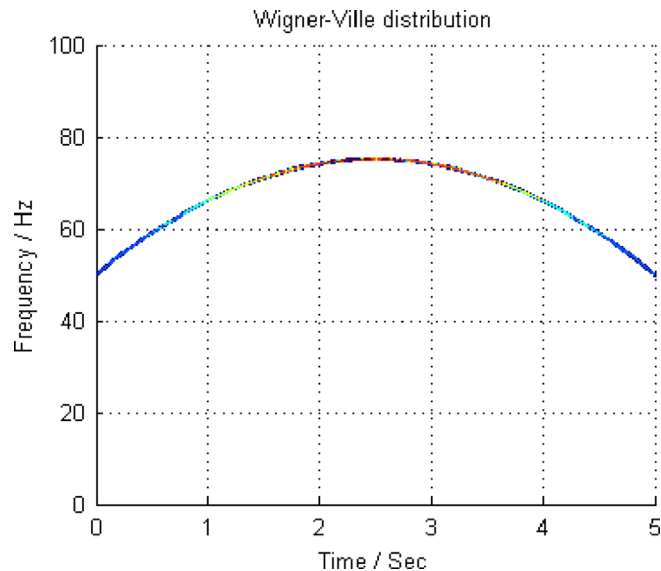


Fig. 7. The novel method's WVD after signal extending.

Table 3

Estimation error of the proposed method after signal extension.

Criterion	ξ_1	ξ_2
Value	2.17%	4.63e3

Acknowledgement

The authors are grateful to the support by the National Natural Science Foundation under Grants 51105243 and 51035007.

The author wishes to thank Curtis Condon, Ken White, and Al Feng of the Beckman Institute of the University of Illinois for the bat data and for permission to use it in this paper and are grateful to the anonymous reviewers for their constructive criticism and valuable comments as they have improved the quality of this paper.

Appendix A. Supporting information

Supplementary data associated with this article can be found in the online version at <http://dx.doi.org/10.1016/j.ymssp.2013.08.010>.

References

- [1] G. Dong, J. Chen, Noise resistant time frequency analysis and application in fault diagnosis of rolling element bearings, *Mechanical Systems and Signal Processing* 33 (2012) 212–236.
- [2] H. Castillejos, et al., Wavelet transform fuzzy algorithms for dermoscopic image segmentation, *Computational and Mathematical Methods in Medicine* 2012 (2012) 578721.
- [3] K. Sudha, et al., Soil characterization using electrical resistivity tomography and geotechnical investigations, *Journal of Applied Geophysics* 67 (2009) 74–79.
- [4] O. Abbasi, et al., Identification of exonic regions in DNA sequences using cross-correlation and noise suppression by discrete wavelet transform, *BMC Bioinformatics* 12 (2011) 430.
- [5] J.R. Carson, T.C. Fry, Variable frequency electric circuit theory with application to the theory of frequency modulation, *Bell System Technical Journal* 16 (1937) 513–540.
- [6] B. Van der Pol, The fundamental principles of frequency modulation, *Journal of the Institution of Electrical Engineers-Part III: Radio and Communication Engineering* 93 (1946) 153–158.
- [7] B. Boashash, Estimating and interpreting the instantaneous frequency of a signal. I. Fundamentals, *Proceedings of the IEEE* 80 (1992) 520–538.
- [8] B. Boashash, Estimating and interpreting the instantaneous frequency of a signal. II. Algorithms and applications, *Proceedings of the IEEE* 80 (1992) 540–568.
- [9] J.W. Cooley, J.W. Tukey, An algorithm for the machine calculation of complex Fourier series, *Mathematics of Computation* 19 (1965) 297–301.
- [10] N.E. Huang, Z. Wu, A review on Hilbert–Huang transform: method and its applications to geophysical studies, *Reviews of Geophysics* 46 (2008) RG2006.
- [11] K. Gröchenig, Describing functions: atomic decompositions versus frames, *Monatshefte für Mathematik* 112 (1991) 1–42.
- [12] H. Hariharan, et al., Image fusion and enhancement via empirical mode decomposition, *Journal of Pattern Recognition Research* 1 (2006) 16–32.

- [13] T. Wang, et al., Comparing the applications of EMD and EEMD on time–frequency analysis of seismic signal, *Journal of Applied Geophysics* 83 (2012) 29–34.
- [14] J. Lerga, V. Sucic, Nonlinear IF estimation based on the pseudo WVD adapted using the improved sliding pairwise ICI rule, *IEEE Signal Processing Letters* 16 (2009) 953–956.
- [15] P. Flandrin, B. Escudié, An interpretation of the pseudo-Wigner–Ville distribution, *Signal Processing* 6 (1984) 27–36.
- [16] D.-f. Ping, et al., Cross-term suppression in the Wigner–Ville distribution using beamforming, in: *Fourth IEEE Conference on Industrial Electronics and Applications*, 2009. ICIEA 2009, pp. 1103–1105.
- [17] Y.-P. Cai, et al., WVD cross-term suppressing method based on empirical mode decomposition, *Jisuanji Gongcheng/Computer Engineering* 37 (2011) 271–273.
- [18] G.-S. Hu, F.-F. Zhu, An improved Chirplet transform and its application for harmonics detection, *Circuits and Systems* 2 (2011) 107–111.
- [19] F. Millioz, M. Davies, Sparse detection in the Chirplet transform: application to FMCW radar signals, *IEEE Transactions on Signal Processing* 60 (2012) 2800–2813.
- [20] F. Kerber, et al., Attenuation analysis of Lamb waves using the Chirplet transform, *EURASIP Journal on Advances in Signal Processing* 2010 (2010) 5.
- [21] S. Mann, S. Haykin, The Chirplet transform: a generalization of Gabor’s logon transform, *Vision Interface* (1991) 205–212.
- [22] Z. Peng, et al., Polynomial Chirplet transform with application to instantaneous frequency estimation, *IEEE Transactions on Instrumentation and Measurement* 60 (2011) 3222–3229.
- [23] S. Mann, S. Haykin, The Chirplet transform: physical considerations, *IEEE Transactions on Signal Processing* 43 (1995) 2745–2761.
- [24] Y. Yang, et al., Spline-kernelled Chirplet transform for the analysis of signals with time-varying frequency and its application, *IEEE Transactions on Industrial Electronics* 59 (2012) 1612–1621.
- [25] C. Li, M. Liang, Time–frequency signal analysis for gearbox fault diagnosis using a generalized synchrosqueezing transform, *Mechanical Systems and Signal Processing* 26 (2012) 205–217.
- [26] D. Malnar, et al., A cross-terms geometry based method for components instantaneous frequency estimation using the Cross Wigner–Ville distribution,” in: *11th International Conference on Information Science, Signal Processing and their Applications (ISSPA)*, 2012, pp. 1217–1222.
- [27] R. Baraniuk, Bat Echolocation Chirp, DSP Group, Rice University, Houston, TX, 2009 (<http://dsp.rice.edu/software/bat-echolocation-chirp>) ([online], available).
- [28] Y. Yang, et al., Multicomponent signal analysis based on polynomial Chirplet transform, *IEEE Transactions on Industrial Electronics* 60 (2013) 3948–3956.